Received: 20 May 2024 | Revised: 18 September 2024 | Accepted: 26 September 2024

DOI: 10.1002/inf2.70004

RESEARCH ARTICLE

WILEY

Adaptive respiratory muscle trainer based on hybrid nanogenerator sensor and artificial intelligence

Ziao Xue[1,2] | Puchuan Tan[2] | Jiangtao Xue[2,3] | Yuan Xi[2,4] | Minghao Liu[2] | Yang Zou[2,3] | Qiang Zheng[5] | Zhou Li[2,6,7] | Yuxiang Wu[1,2,8]

[1]Institute of Intelligent Sport and Proactive Health, Department of Health and Physical Education, Jianghan University, Wuhan, the People's Republic of China

[2]Beijing Institute of Nanoenergy and Nanosystems, Chinese Academy of Sciences, Beijing, the People's Republic of China

[3]School of Medical Technology, Beijing Institute of Technology, Beijing, the People's Republic of China

[4]Key Laboratory of Biomechanics and Mechanobiology of Ministry of Education Advanced Innovation Center for Biomedical Engineering School of Engineering Medicine, Beihang University, Beijing, the People's Republic of China

[5]Engineering Research Center of Intelligent Materials and Advanced Medical Devices, School of Biology and Engineering, Guizhou Medical University, Guiyang, the People's Republic of China

[6]School of Nanoscience and Engineering, University of Chinese Academy of Sciences, Beijing, the People's Republic of China

[7]College of Chemistry and Chemical Engineering, Center on Nanoenergy Research, Guangxi University, Nanning, the People's Republic of China

[8]College of Sports Medicine, Wuhan Sports University, Wuhan, the People's Republic of China

Correspondence

Qiang Zheng, Engineering Research Center of Intelligent Materials and Advanced Medical Devices, School of Biology and Engineering, Guizhou Medical University, Guiyang 561113, the People's Republic of China.
Email: zhengqiang@gmc.edu.cn

Zhou Li, Beijing Institute of Nanoenergy and Nanosystems, Chinese Academy of Sciences, Beijing 101400, the People's Republic of China.
Email: zli@binn.cas.cn

Yuxiang Wu, Institute of Intelligent Sport and Proactive Health, Department of Health and Physical Education, Jianghan University, Wuhan 430056, the People's Republic of China.
Email: yxwu@jhun.edu.cn

Funding information

National Key R&D Project from the Minister of Science and Technology, Grant/Award Number: 2023YFB3208101; National Natural Science Foundation of China, Grant/Award Number: T2125003; National Key R&D Program of China,

Abstract

Respiratory muscle training can improve respiratory function by strengthening muscle mass, which is of great help to populations with respiratory system diseases and athletes. Existing respiratory muscle training methods rely on resistance that hinders breathing, and the resistance cannot be adjusted automatically. However, the detection of the user's current muscle fatigue state and precise adjustment of resistance during respiratory muscle training are crucial to training efficiency. Here, we have developed a hybrid sensor that combines a triboelectric nanogenerator and a piezoelectric nanogenerator. This hybrid sensor can simultaneously collect both high-frequency and low-frequency signals generated by the Karman vortex street effect with low hysteresis. When the airway height is 30 mm, the sensor size is 52 μm × 40 mm × 17 mm, the output performance of the sensor is optimal, and the minimum response amplitude for the sensor is approximately 3 mm. Under normal breathing conditions, the output peak voltage is 7 V, the current is 100 μA, the charge transfer amount generated by one movement is 55 nC, the response time is 0.16 s, and the sensitivity is 0.07 V/m·s^{-1}. With the help of the principal component analysis algorithm, features related to the fatigue state of muscles were extracted from the collected signals, and the accuracy rate can reach 94.4%. Subsequently, the stepper motor will rotate to adjust the

Grant/Award Number: 2022YFE0111700; China Postdoctoral Science Foundation, Grant/Award Number: 2023M743446; Science Fund for Distinguished Young Scholars of Hubei Province, Grant/Award Number: 2023AFA109; Guizhou Provincial Basic Research Program (Natural Science), Grant/Award Number: ZK2023-032; Guizhou Provincial Key Technology R&D Program, Grant/Award Number: 2024161; Fundamental Research Funds for the Central Universities

resistance appropriately. We fused the hybrid sensor, machine learning, control circuits, and stepper motors and fabricated a resistance self-adaptation program. Our findings inspire researchers in the field of rehabilitation and sports training to evaluate training status and improve training efficiency.

KEYWORDS

artificial intelligence, hybrid, nanogenerator sensor, respiratory sensor, self-adaptation

1 | INTRODUCTION

Respiration is the process of gas exchange between the organism and the external environment that helps us take in oxygen, metabolize waste, and is one of our vital signs. Respiration is the basis of pulmonary ventilation, which in turn involves inhalation and exhalation. In order to achieve inhalation and exhalation, we use a series of muscles such as the diaphragm, intercostal muscles, rectus abdominis, and others to help the lungs fill and contract to maximize the inhalation and exhalation of gases.[1] During inspiration, contraction of the diaphragm causes the diaphragm dome to descend and the thoracic cavity volume to expand to assist inspiration. During expiration, relaxation of the septum muscle causes the diaphragm dome to rise and return to its original position, while the rectus abdominis muscle contracts, and the thoracic cavity volume decreases to assist expiration.[2] These muscles which are used for respiratory are collectively known as "respiratory muscles" Just like other skeletal muscles in our body, the "respiratory muscles" can be enhanced physiologically (muscle cross-sectional area[3]), reflected in the increase of respiratory muscle strength[4] and endurance,[5] that allows for easier and more effective ventilation and function effectively without fatigue during longer periods of physical activity. Another enhancement is respiratory patterns, that improve body posture while enhancing pulmonary ventilation efficiency, improving function and efficiency. As respiration is very closely related to athletic performance, respiratory muscle training can even improve athletic performance to some extent and even reduce the complications of some diseases,[6–8] it is helpful for people who have weakened respiratory function[9]/suffer from certain respiratory diseases[9,10] or athletes, and so forth.[11]

Currently, respiratory muscle training is performed using resistance training, which increases the resistance that the respiratory muscle groups have to overcome during inhalation or exhalation, and is divided into inspiratory and expiratory muscle training.[12] Respiratory muscle training is usually preceded by testing the user's maximal inspiratory pressure (MIP) and maximal expiratory pressure (MEP) using a measuring device and determining the training load in terms of the percentage index of MIP and MEP.[13] In the process of the MIP and MEP test, maximum strength contraction and relaxation of respiratory muscles may cause hyperventilation, which is not friendly to elders. In addition, MIP and MEP have more correlation with individual differences, health status, and physical activity habits, which leads to a larger range of differences in MIP and MEP among the elderly.[14] Therefore, MIP and MEP should be measured and interpreted with more caution. There are several commercially available respiratory resistance trainers on the market, but some of them still have disadvantages in portability, usability, adjustable.[15] These problems affect the effectiveness and efficiency of respiratory muscle training. To improve effectiveness and efficiency, the physical signal of respiration, flow, needs to be quantified.[16] Current respiratory sensors include both flow sensors (which quantify airflow through the mouth[17] and nose[18]) and strain sensors (which quantify the rise and fall of the chest,[19] abdomen[20] and other part as a result of respiration).[21] The former is relatively direct and the latter is relatively indirect. For respiratory flow monitoring, many people use triboelectric sensors to achieve self-powered operation while monitoring respiratory frequency and depth. Self-powered sensors can eliminate dependence on external power sources, which is beneficial for further reducing the size of the device. Swinging respiratory sensors[22] often adopt a single-electrode model; the two friction layers will repeatedly contact and separate through the vortex generated by breathing that achieving monitoring of respiratory flow rate. Liu[17] reported a floating rotary freestanding TENG, where the friction layers are respectively placed on the stator and rotor. When the airflow passes through, the rotor rotates and generates triboelectrical signals due to electrostatic induction. Strain sensors such as polyvinylidene difluoride (PVDF) can also be used to monitor respiratory rate and depth. PVDF piezoelectric material for sensing respiratory airflow is placed on the mask to improve user wear

comfort.[18] It can be hybridized with triboelectric sensors to improve the output of the sensor to improve the output of the sensor, Zou[20] designed a hybrid sensor inspired by shark gills for wearable respiratory monitoring, which is stretchable due to the flexible substrate and shark gill structure. Sensors with a turbine structure are representative flow sensors and are commonly used for spirometry, but they have the disadvantage of hysteresis due to the rotational inertia of the turbine.[23] Therefore, the development of a respiratory muscle trainer that accurately quantifies respiratory status, automatically adjusts resistance, and is portable is critical.

In order to solve the hysteresis of the vortex fan flowmeter, using the Karman vortex street effect,[24] we designed a hybrid sensor, which fixes two pieces of polyvinylidene difluoride (PVDF) symmetrically on the support structure. When the airflow passes, both sensors start to work, and when the airflow stops, both sensors stop working immediately; this effect solves the hysteresis problem of respiratory sensing. In addition, the sensing array has the advantages of collecting rich, accurate, and stable information. The individual hybrid sensors are fabricated based on the properties of triboelectric nanogenerators (TENG)[25,26] and piezoelectric nanogenerators (PENG).[27] As a self-powered sensor,[28] TENG has attracted much attention due to its advantages of high sensitivity,[21] high responsiveness,[28] and low cost.[29] Unlike TENG, PENG has a stronger ability to perceive deformation and is more suitable for sensing low-frequency signals.[30] Hybrid sensors based on TENG and PENG have the ability to sense high-frequency signals versus low-frequency signals at the same time, enriching the respiratory information sensed. It is capable of recognizing different respiratory frequencies, depths, and durations. The sensor array makes it possible to always have a piece of the sensor as a control sensor while respiration, enabling more accurate dual-channel sensing. The hybrid sensor shows good durability and remains stable after 5000 airflow cycles.

We fused a hybrid sensor, machine learning (ML),[31,32] control circuits, stepper motors, and fabricated a Resistance Self-Adaption Program (RSP). This program automatically matches the user with the current appropriate resistance, making our respiratory muscle trainer intelligent. We have recruited a group of volunteers to collect data on the respiratory signals at different resistances. After completing the data collection, ML algorithms were used to build a library of data models to classify and quantify the respiratory signals for assessing the user's perception and determine the resistance match, with a final ML recognition rate of 94.4%. When the user uses the RSP for respiratory training, the main-control chip will analyze and judge the data obtained from the respiratory sensing array, if the RSP determines that the current user's ability matches the gear level, the stepper motor will not rotate. If the RSP determines and sends a resistance adjustment command (clockwise or anticlockwise) to the stepper motor, the stepper motor will rotate to adjust the resistance until the RSP determines that the current user's ability matches the gear level. In addition, the system can also evaluate the user's respiratory function to determine the effectiveness of long-term training. In brief, the intelligent respiratory muscle trainer based on the sensing array and RSP has the function of combining evaluation and training regulation and shows a good trend and future application prospect in respiratory muscle training and respiratory function improvement.

2 | RESULTS AND DISCUSSION

2.1 | Material and structure

As the Figure 1A shows, the overall structure of the intelligent respiratory muscle trainermainly includes the sensing part, resistance part, circuit, and control part. The sensing part mainly consists of Polyethylene terephthalate (PET) cover plates, polylactic acid (PLA) frame, a polytetrafluoroethylene (PTFE) film, and two PVDF films. Seal the upper and lower ends of the support with PET cover plates to form air ducts that allow airflow to pass. The PENG sensor uses soft piezoelectric material PVDF as the functional material and is fixed in the support of PLA printing. The surface of PVDF is coated with a layer of Ag as the electrode, which tends to have a positive triboelectric sequence and is prone to losing electrons. PTFE is a material that tends to have a negative triboelectric sequence and is easy to obtain electrons. In order to enhance the triboelectric effect generated by PVDF during oscillation, PTFE tape is attached to the inner side of the PET cover plate above. This way, when PVDF undergoes oscillation due to airflow, the Ag on the surface of PVDF can produce a good triboelectric effect with the PTFE film. As shown in the bottom right corner of Figure 1A, the sensor will present four working states with respiration, namely inhalation state, breath holding state, exhalation state, and breath holding state.

The resistance part is composed of a commercial respiratory muscle damping part, which is specifically a one-way valve supported by springs. When the suction force is sufficient to overcome the spring force, the valve opens, and when the suction force gradually weakens, the valve closes. The fixed structure of the rotating spring can adjust the length of the compressed spring, and the resistance that needs to be overcome is also adjusted accordingly. By the one-way valve resistance system we used, the users could overcome resistance during

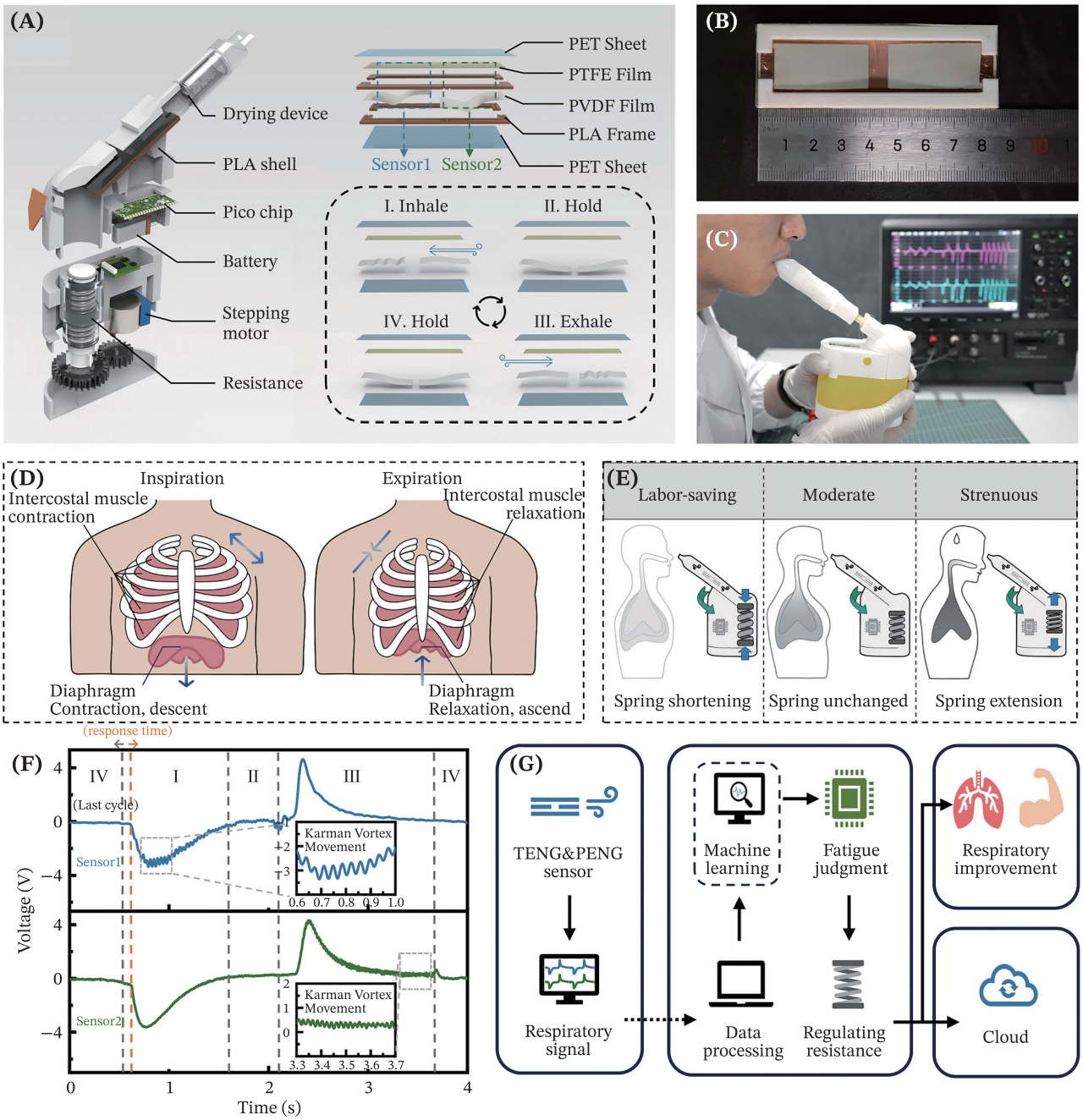

FIGURE 1 The overview of resistance adaptive respiratory trainer. (A) Schematic diagram of the sensor part and supporting part of the intelligent respiratory trainer. (B) The optical photo of the hybrid nanogenerator sensor. (C) Application of the respiratory muscle training device in human body demonstration. (D) Schematic diagram of intercostal and diaphragmatic muscle movements during exhalation/inhalation. (E) The working status of RSP under labor-saving condition, moderate condition, and strenuous condition. (F) The voltage signal of a respiratory cycle. (G) The design concept of the intelligent respiratory trainer.

inhalation and not during exhalation. This can enable the relevant muscle groups that assist in inhalation to achieve resistance exercises. Subsequently, we implemented an adaptive resistance function using machine learning-based judgment methods. Figure 1B shows the optical photo of a hybrid nanogenerator sensor. Figure 1C shows an example of a user exercising with our intelligent respiratory muscle trainer. When the human respiratory, the relevant muscle group will contract or relax; Figure 1D shows this situation. Specifically, when a person inspires, the intercostal muscle contracts, the diaphragm muscle contracts and descends, and the chest cavity expands; when a person expires, the intercostal muscle relaxes, the diaphragm muscle relaxes and

ascends, and the chest cavity shrinks. As Figure 1E shows, the specific situation is as follows: when used in a gear level that is judged to be moderate (i.e., with good training effect), the stepper motor will not rotate, the spring length will not change, and the resistance will not change in any way. When the user's signal is judged to be labor-saving, the stepper motor will rotate to shorten the spring, and the resistance will increase accordingly. When the user's signal is judged to be strenuous, the stepper motor will rotate to extend the spring, and the resistance will decrease accordingly.

The circuit consists of a main-control chip (Raspberry Pi PICO), a stepper motor, a stepper motor driver board, button switches, and two lithium batteries. When the user is training, the main-control chip is responsible for receiving the generated respiratory signal from the sensor. These signals are processed by the main-control chip; it will send instructions to the stepper motor to adjust the resistance. Through the self-adaptive resistance function of the RSP, users can receive better training results. The four states corresponding to the electrical signals during the respiratory cycle are shown in Figure 1F. Significantly, the two sensors generate corresponding high-frequency signals in periods II and IV, respectively. These high-frequency signals are generated due to the Karman vortex street generated by exhalation or inhalation. The response time shows the retardation of the sensor (Figure S1). In addition, we envision uploading training data to the cloud for users to analyze and develop exercise plans. Figure 1G shows the design concept of our manufactured intelligent respiratory muscle trainer.

2.2 | Characterization and optimization

When a fluid bypasses certain objects under certain conditions, such as flow velocity, object size, and fluid properties, the two sides of the object will periodically shed double row line vortices with opposite rotation directions and regular arrangements; this phenomenon is called the Karman vortex street effect.[33] Inspired by the effect, we designed and fabricated this sensor array. Figure 2 shows the characterization of the sensor. PVDF is a material with a piezoelectric effect, which has the characteristics of lightweight, flexibility, and can be easily bent. PVDF films were selected as the oscillating layer for the Karman vortex street, and the airflow generated by respiration bends the PVDF to generate piezoelectric polarization charges,[34] which generate piezoelectric signals. Due to the triboelectric effect,[35] the surface of the PVDF film and PTFE film have opposite polarity triboelectric charges. The vortex causes the PVDF film to separate from the repeated contact with the PTFE film and generates triboelectric induced charges on the electrodes at the PVDF film, which generates triboelectric signals. In this way, the triboelectric and piezoelectric signals were combined. The advantage of hybrid is that it can simultaneously collect piezoelectric signals and triboelectric electrical signals generated by the airflow. Due to our symmetrical placement, two PVDF films can generate periodic oscillations due to the vortex generated during exhalation or inhalation, respectively. Therefore, our sensor can collect hybrid signals during the respiratory process.

To verify the working principle of the sensor, the finite element analysis shows structural deformation of the sensor under vortex Kármán conditions; the tested voltage output also reflects the structural deformation of the sensor under a respiratory cycle (Figure S2). As Figure 2A–C shows, the voltage, current, and charge of a single sensor were characterized, with a peak voltage of 7 V and a peak current of 100 μA. Its single charge transfer amount is 55 nC.

Environmental noise is a factor that constrains the performance of sensors and objectively affects the signal-to-noise ratio.[36] As environmental noise is usually unchanging, the signal-to-noise ratio can be improved by increasing the output of the sensor.[37] Therefore, it is necessary to find the most suitable size to optimize the output of the sensor. There have three factors affect output: the thickness, length of the PVDF, and the cross-sectional height of the flow channel. As the Figure 2D shows, when the thickness of PVDF film is 52 μm, the signal output is highest. The output of different PVDF films lengths was measured in the same cross-sectional height of the flow channel and results showed that there was close in the output of PVDF films within the length range of 40, 38, 36 mm (Figure 2E). To confirm whether the cross-sectional height of the flow channel affects the voltage output, voltage output of sensor was tested under five different cross-sectional heights (10 mm, 20 mm, 30 mm, 40 mm, and 50 mm). As Figure 2F shows, the cross-sectional height has little effect on the output of PVDF, so 3 mm cross section height was selected as a solution. Finally, PVDF film size of 52 μm × 40 mm × 17 mm was selected, and the sensor's channel height was set to 3 mm. The sensor made with this parameter has the optimal signal output and signal-to-noise ratio that was used for subsequent characterization testing. Figure S3 shows that the minimum response amplitude for the sensor is approximately 3 mm. Figure 2G shows the quadratic equation relationships of sensor peak voltage output and wind speed. When the wind speed is between 0 and 5 m s^{-1}, the sensitivity of sensor is 0.07 V/m·s^{-1}, while the wind speed is between 5 and 15 m s^{-1}, the sensitivity of sensor is −1.87 V/m·s^{-1}.

The gas exhaled by the human body is accompanied by a certain humidity that has a huge impact on

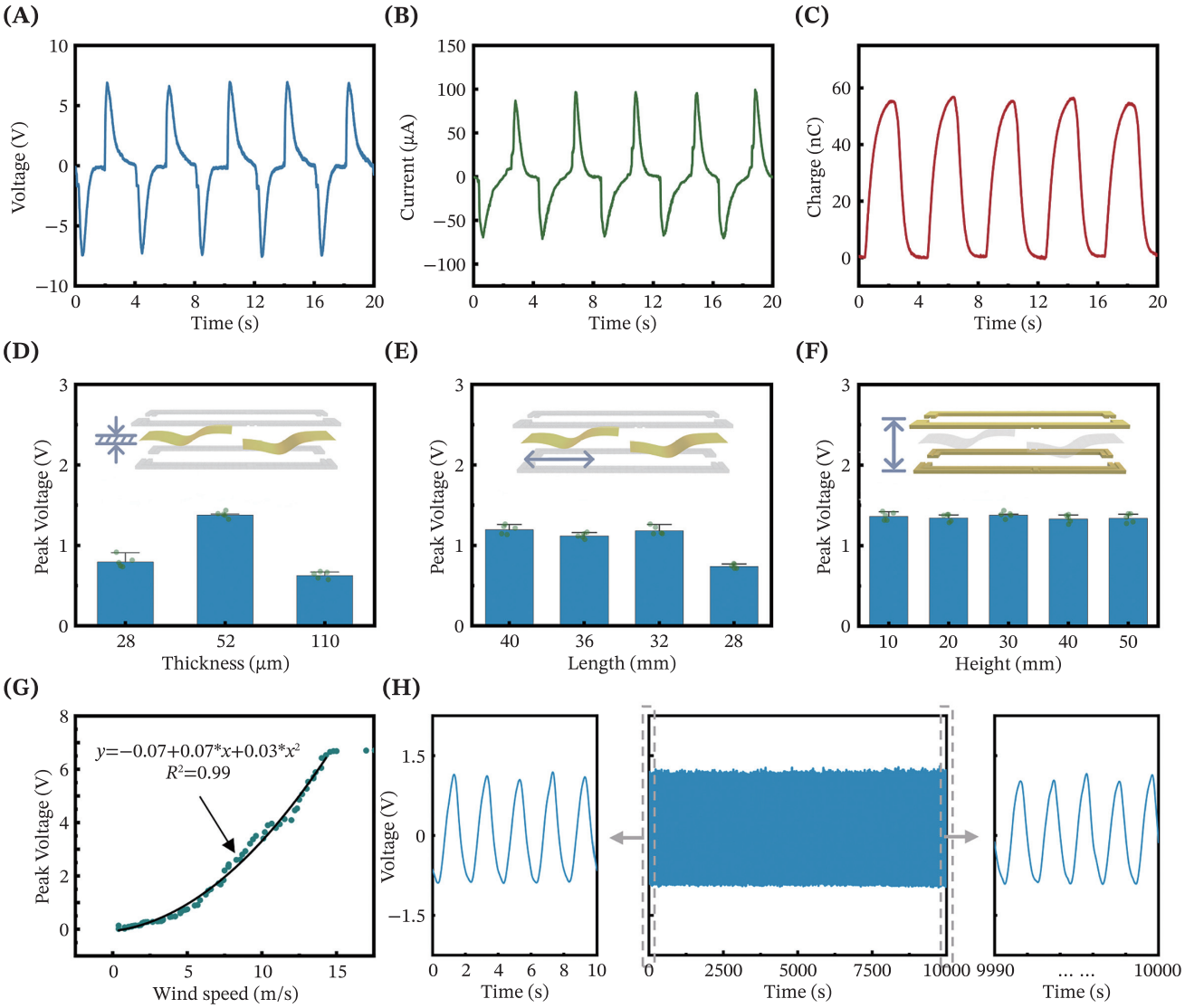

FIGURE 2 The characterization of the sensor. (A) The voltage signal diagram of three respiratory cycles of the sensor. (B) The current signal diagram of three respiratory cycles of the sensor. (C) The charge signal diagram of three respiratory cycles of the sensor. (D) The peak voltage of the sensor under different PVDF film thickness conditions. (E) The peak voltage of the sensor under different channel height conditions. (F) The peak voltage of the sensor under different PVDF film length conditions. (G) The relationship of the sensor peak voltage output and wind speed. (H) The voltage signal diagram of 5000 times airflow cycles of the sensor.

triboelectricity. In order to address the impact of humidity on sensors, we adopted a strategy of reducing the humidity of exhaled gas and designed and manufactured an air dryer (Figure S4). This air dryer uses absorbent resin as a desiccant to reduce the humidity of exhaled moist gas after passing through it. Moreover, the stability of the hybrid sensor was tested under dry conditions under 5000 cycles within 10,000 s. The cycle test wind speed is 7 m s^{-1}, which is close to the wind speed of human-exhaled air. As shown in Figure 2H, the stable voltage signal indicates that the sensor has long-term durability. The effectiveness of our strategy to reduce exhaled gas humidity was also verified in the subsequent stage of collecting human respiratory signals.

The Karman vortex street effect leads to repeated contact and separation between PVDF vibration and PET. Due to the potential difference between the surfaces of the two materials, repeated contact and separation cause the transfer of surface charges, resulting in a triboelectric contact electrification phenomenon. PTFE film was applied to the cover plate to enhance the triboelectricity generated by contact separation. PTFE is a material that is easy to obtain electrons. The surface of the PVDF film is coated with a layer of silver electrode, which is a material that is prone to losing electrons. When PTFE rubs

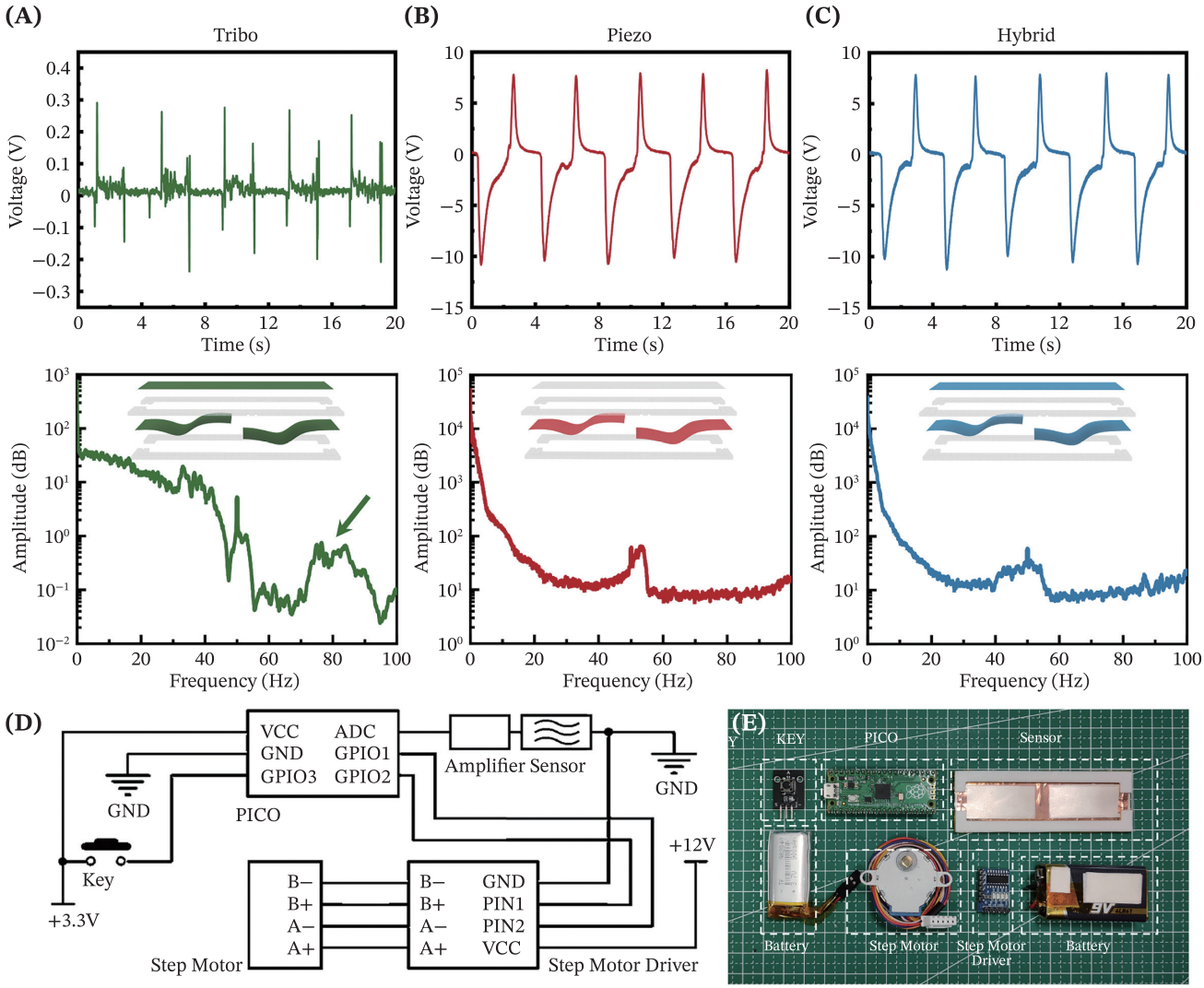

FIGURE 3 The comparison of pure triboelectric sensor, pure piezoelectric sensor, hybrid sensor, and circuit design of resistance self-adaptive respiratory muscle trainer. (A) Voltage signal diagram and frequency diagram of a pure triboelectric sensor. (B) Voltage signal diagram and frequency diagram of a pure piezoelectric sensor. (C) Voltage signal diagram and frequency diagram of a hybrid sensor. (D) Circuit diagram of the respiratory muscle trainer. (E) The optical photo of electronic components for the respiratory muscle trainer.

against Ag, an electrical signal can be generated. When the airflow passes through the device, under the Karman vortex street effect, two PVDF films will experience periodic swings. With the periodic swing of the PVDF film, PTFE will repeatedly contact and separate from the PVDF film, resulting in friction between PTFE and Ag, leading to regular triboelectric signals. Meanwhile, due to PVDF being a piezoelectric material, when it undergoes deformation under external forces, it will generate a piezoelectric signal output. Figure 3A–C compares the voltage signal outputs of pure triboelectric, pure piezoelectric, and hybrid sensors under the same structural size. We present their respective frequency domain diagrams obtained through Fourier transform. As shown in the figure, the triboelectric sensor mainly collects wide-frequency signals during respiration, while the piezoelectric structure mainly collects low-frequency signals during respiration. The combination of triboelectric and piezoelectric signals expands the frequency domain range of hybrid sensors, reflecting their advantages in information perception during respiration. Figure 3D shows the circuit design of the resistance adaptive respiratory muscle trainer. Figure 3E shows the optical photo of electronic components for the respiratory muscle trainer.

2.3 | Signal processing and model establishment

The respiratory signal is affected by various conditions and will produce various waveforms. Among them,

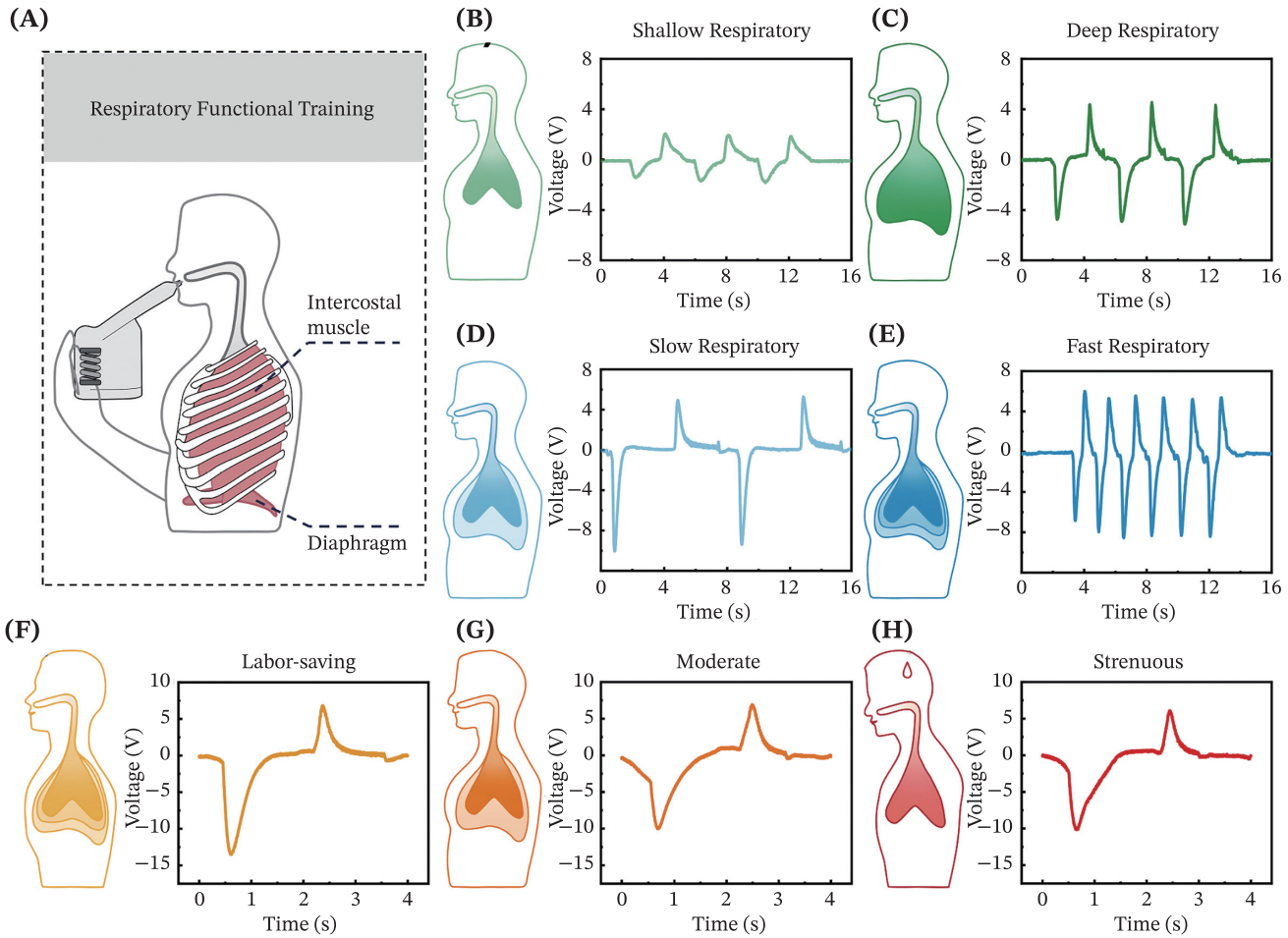

FIGURE 4 The application of intelligent respiratory muscle trainer. The sensor can show respiratory depth, respiratory frequency, and fatigue level. (A) Schematic diagram of respiratory muscle training and related muscle groups. (B–E) Voltage signal diagram of shallow respiratory, deep respiratory, slow respiratory, and fast respiratory. (F–H) Voltage signal diagram of labor-saving, moderate, and strenuous states, respectively.

factors that have a greater impact on respiration signals include individual differences, respiration resistance, and the user's physiological state. The muscles that assist in inhaling/exhaling may experience fatigue due to changes in resistance and duration of inhalation/exhalation, and fatigue is usually only subjectively felt by the human body, making it difficult for others to observe.[38] Moreover, due to differences in individual subjective tolerance for fatigue, the accuracy of subjective judgment of fatigue will decrease. There are two types of muscle fiber in skeletal muscle, type I muscle fibers and type II muscle fibers. Type I muscle fibers are mainly aerobic metabolism with low output power and fatigue resistance, while type II muscle fibers are mainly anaerobic metabolism with high output power and are prone to fatigue.[39,40] When conducting resistance training for respiratory muscles, type II muscle fibers need to be recruited. When type II muscle fibers are fatigued, the power output of muscle will significantly decrease, the muscle contraction speed will slow down, and the muscle contraction will be uncoordinated, manifested in a decrease in inspiratory/expiratory volume and an increase in respiratory instability. Our hybrid sensor can collect rich information, which can directly perceive the depth, rate, and signal frequency of respiratory. These information can be analyzed to determine the current fatigue state of respiratory muscles. Figure 4A shows a schematic diagram of respiratory-related muscle groups undergoing resistance training using our intelligent respiratory muscle trainer. Figure 4B–H and Movies S1-2 show that our sensors can well record data signals such as the depth, speed, and fatigue status of respiration. Calculating better analysis results requires recording more respiratory data, increasing the sampling rate, and increasing the recording time of the signal. The variation characteristics of signals in different individuals or resistance states can be collected. However, these large amounts of across-individual data exacerbate the difficulty of manual analysis. Therefore, it

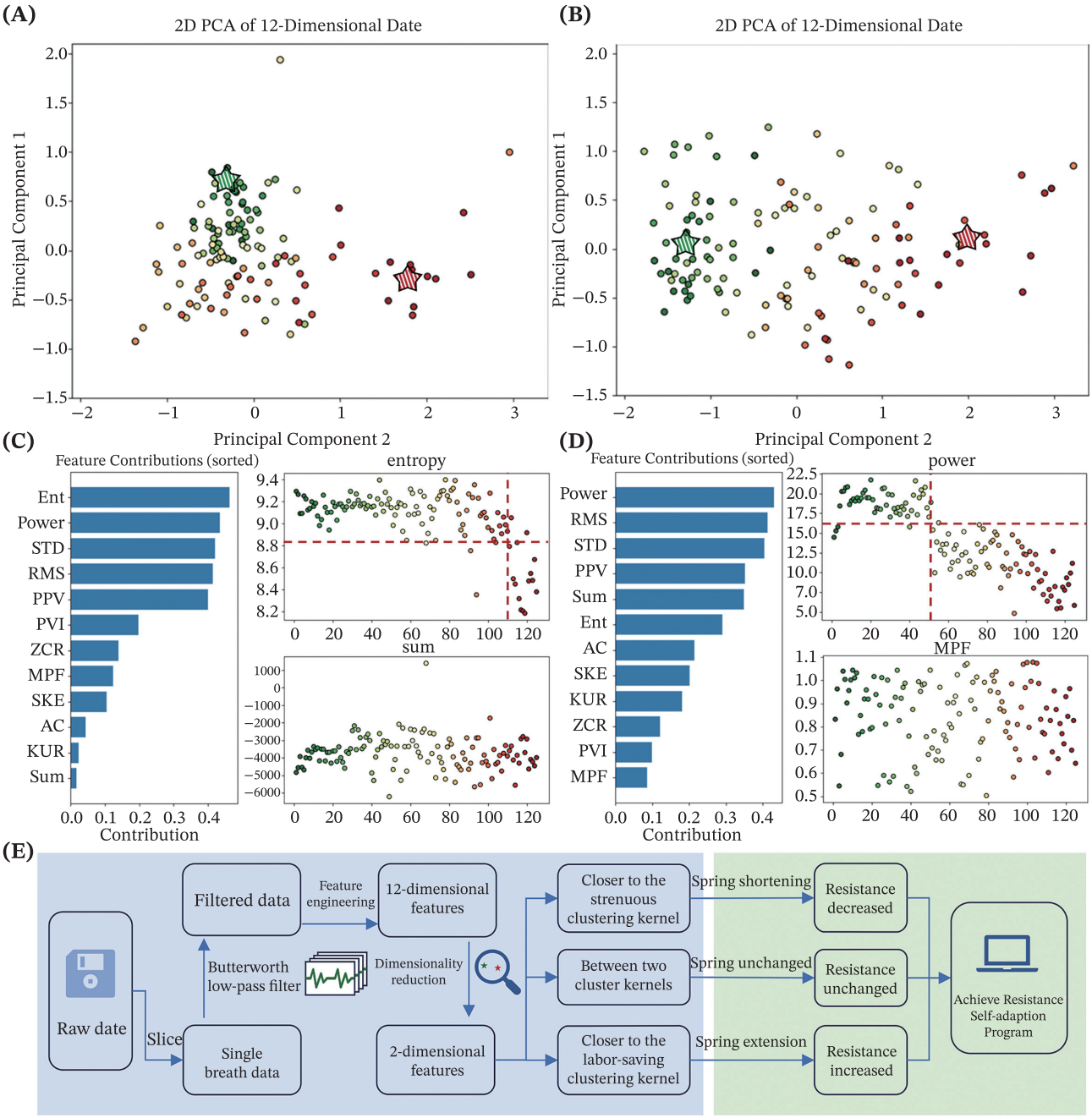

FIGURE 5 2-D PCA of 12-D date diagram of resistance inhalation and no resistance exhalation and its characteristic contribution rate. (A) 2-D PCA of 12-D date diagram of 125 times no resistance exhalation, each spot represents a sample, and the pentagram represents a cluster center. (B) 2-D PCA of 12-D date diagram of 125 times resistance inhalation. (C) The different features contribution of 125 times no resistance exhalation. (D) The different features contribution of 125 times resistance inhalation. (E) Flow diagram of machine learning for RSP of intelligent respiratory muscle trainer.

is necessary to use machine learning methods to reduce the burden of human data processing.

In order to distinguish and judge the respiratory data of fatigue principal component analysis (PCA) was used to process and analyze respiratory data. PCA is the most widely used data dimensionality reduction algorithm. The principle of PCA is to map n-dimensional features onto k-dimensional features, which are brand new orthogonal features also known as principal components.[29,41] The data were collected from 125 consecutive breaths (Figure 5A,B). As the times of respiratory increases, fatigue gradually appears. To distinguish the respiratory signals of fatigue, the dimensionality of 12 features was reduced, which are Standard Deviation (STD),

Entropy (Ent), Autocorrelation Coefficient (AC), Zero Cross Rate (ZCR), Power, Root Mean Square (RMS), Sum, Peak to Peak Value (PPV), Peak Valley Interval (PVI), Kurtosis (KUR), Skewness (SKE), Mean Power Frequency (MPF) and finally obtained the contribution of different features. Resistance was only set in the inhalation channel, while the exhalation channel has almost no resistance. So, the fatigue in the inhalation stage will come earlier. As shown in Figure 5C, for exhalation, the entropy value is a feature that is more effective in distinguishing fatigue from non-fatigue, and fatigue appears after 110 exhalations. For inhalation, power is a characteristic used to distinguish between fatigue and non-fatigue (Figure 5D), and fatigue appeared during the 50th inhalation. Finally, the level of respiratory muscle fatigue was graded through these features. Figure 5E presents a flowchart showing machine learning for RSP of the intelligent respiratory muscle trainer. Initially, the raw data of respiratory were collected. After the data slice, filtering process, feature extraction and selection, the 12-dimensional features were reduced to 2-dimensional features. Then the machine learning model was established between the feature matrices. The respiratory situations can be distinguished by features into strenuous, normal, labor-saving; subsequently, the spring will shorten, remain unchanged, or extend. The resistance self-adaptation program achieved as above (Movie S3).

3 | CONCLUSION

In summary, we have designed a respiratory muscle trainer based on machine learning and a hybrid nanogenerator sensor. The hybrid nanogenerator sensor can effectively identify the user's respiratory depth, respiratory frequency, and fatigue level. The peak voltage of the hybrid nanogenerator sensor can reach 7 V, and the response time can be reduced to 0.16 s due to the Karman vortex street effect. Moreover, due to the unique characteristics of triboelectric nanogenerators and piezoelectric nanogenerators, hybrid nanogenerator sensors have a wide sensing range and can collect both high-frequency and low-frequency signals of respiration. In order to achieve automatic resistance adjustment that is compatible with the respiratory state, we have developed a RSP that can determine the user's respiratory state through sensors. The data analyzed by the PCA algorithm can be used to determine whether to send resistance adjustment instructions to the stepper motor, thereby keeping the resistance at an acceptable level for the user, and the average accuracy for fatigue state recognition is 94.4%. Our respiratory muscle trainer demonstrates an example of sensing and adaptive resistance regulation, which is expected to be applied in respiratory muscle training and improve training efficiency, and extended to other similar applications, demonstrating applications in sports training, post-patient rehabilitation, and other scenarios.

4 | EXPERIMENTAL SECTION

We designed the shell of the respiratory muscle training device using Rhino7 and printed it using PLA material using a 3D printer (Raise 3D, Beijing, China). PVDE comes from VKING Manufacturing Co., Ltd. The main-control board used is from Raspberry Pi Ltd., responsible for collecting signals and making resistance adjustment judgments. Resistance adjustment is achieved through commercial stepper motors and controllers. The power supply uses two commercial lithium batteries. The characterization process of electrical signals was carried out using electrometer (Keithley 6517, Beijing, China) and oscilloscope (LeCroy HDO6104, New York, USA). Using a commercial blower to characterize the wind speed of the device, and connecting the device to the blower through a designed pipeline.

4.1 | Manufacturing of sensors

Cutting PET film to a size of 3 cm × 9.5 cm and a thickness of 1 mm is used as the material for the upper and lower sides, and a PTFE film with a thickness of 0.6 mm is pasted on the inner side of a PET film. Cut two pieces to a size of 1.7 cm × 4 cm, with a thickness of 52 μm and wipe the four edges of each side with an alcohol swab to avoid short circuits and conduction on both sides of the PVDF. The cutting area is 3 mm × 10 mm; double-sided conductive copper tape is used to stick the enameled wire onto the silver electrode layers on both sides of the PVDF. Design and print the supporting structure of PLA material using Rhino7 and a 3D printer (Raise 3D, Beijing, China). Use Kapton double-sided adhesive to stick on both sides of the PLA support material for bonding and fixing with PET film and PVDF, respectively.

4.2 | Characterization and measurement

The oscilloscope (LeCroy, HDO6104, New York, USA) and the Nanogenerator Analyzer (T5000-18A, Beijing, China) are used to measure the hybrid nanogenerator sensor and store data. The Keithley 6517 electrometer is used to measure the current and charge of the hybrid

nanogenerator sensor. The airflow is generated by a blower with airflow (Stanley STPT600, Jinhua, China) for speed control. A timed disconnect device is used to control the duration of each airflow generated by the blower, and a fan blade anemometer (UNI-T, UT363BT, Dongguan, China) is used to monitor the airflow speed in real time.

ACKNOWLEDGMENTS

Ziao Xue and Puchuan Tan contributed equally to this work. The authors are thankful for the support provided by the National Key R&D Project from the Minister of Science and Technology (2022YFE0111700, 2023YFB3208101), the National Natural Science Foundation of China (T2125003), the China Postdoctoral Science Foundation (2023M743446), the Science Fund for Distinguished Young Scholars of Hubei Province (2023AFA109), the Guizhou Provincial Basic Research Program (Natural Science) No. ZK2023-032, the Guizhou Provincial Key Technology R&D Program No. 2024161, and the Fundamental Research Funds for the Central Universities.

CONFLICT OF INTEREST STATEMENT

The authors declare no conflict of interest.

ORCID

Zhou Li https://orcid.org/0000-0002-9952-7296

REFERENCES

1. Reid WD, Dechman G. Considerations when testing and training the respiratory muscles. *Phys Ther*. 1995;75(11):971-982.
2. Pilarski JQ, Leiter JC, Fregosi RF. Muscles of breathing: development, function, and patterns of activation. *Compr Physiol*. 2019;9(3):1025-1080.
3. Pauloski BR, Yahnke KM. Using ultrasound to document the effects of expiratory muscle strength training (EMST) on the geniohyoid muscle. *Dysphagia*. 2021;37(4):788-799.
4. Bissett BM, Leditschke IA, Neeman T, Boots R, Paratz J. Inspiratory muscle training to enhance recovery from mechanical ventilation: a randomised trial. *Thorax*. 2016;71(9):812-819.
5. Fischer G, Tarperi C, George K, Ardigò LP. An exploratory study of respiratory muscle endurance training in high lesion level paraplegic Handbike athletes. *Clin J Sport Med*. 2014;24(1):69-75.
6. Menezes KKP, Nascimento LR, Ada L, Polese JC, Avelino PR, Teixeira-Salmela LF. Respiratory muscle training increases respiratory muscle strength and reduces respiratory complications after stroke: a systematic review. *J Physiother*. 2016;62(3):138-144.
7. van de Wetering-van Dongen VA, Kalf JG, van der Wees PJ, Bloem BR, Nijkrake MJ. The effects of respiratory training in Parkinson's disease: a systematic review. *J Parkinsons Dis*. 2020;10(4):1315-1333.
8. Ramírez-Sarmiento A, Orozco-Levi M, Güell R, et al. Inspiratory muscle training in patients with chronic obstructive pulmonary disease. *Am J Respir Crit Care Med*. 2002;166(11):1491-1497.
9. McNarry MA, Berg RMG, Shelley J, et al. Inspiratory muscle training enhances recovery post-COVID-19: a randomised controlled trial. *Eur Respir J*. 2022;60(4):2103101.
10. Beaumont M, Forget P, Couturaud F, Reychler G. Effects of inspiratory muscle training in COPD patients: a systematic review and meta-analysis. *Clin Respir J*. 2018;12(7):2178-2188.
11. Powers SK, Coombes J, Demirel H. Exercise training-induced changes in respiratory muscles. *Sports Med*. 1997;24(2):120-131.
12. Illi SK, Held U, Frank I, Spengler CM. Effect of respiratory muscle training on exercise performance in healthy individuals a systematic review and meta-analysis. *Sports Med*. 2012;42(8):707-724.
13. Neder JA, Andreoni S, Lerario MC, Nery LE. Reference values for lung function tests. II. Maximal respiratory pressures and voluntary ventilation. *Braz J Med Biol Res*. 1999;32(6):719-727.
14. Evans JA, Whitelaw WA. The assessment of maximal respiratory mouth pressures in adults. *Respir Care*. 2009;54(10):1348-1359.
15. de Menezes KKP, do Nascimento LR, Avelino PR, Polese JC, Teixeira-Salmela LF. A review on respiratory muscle training devices. *J Pulm Respir Med*. 2018;8(2):451.
16. Selyanchyn R, Wakamatsu S, Hayashi K, Lee SW. A nano-thin film-based prototype QCM sensor array for monitoring human breath and respiratory patterns. *Sensors Basel*. 2015;15(8):18834-18850.
17. Liu MH, Tan PC, Xue JT, et al. A portable self-powered turbine spirometer for rehabilitation monitoring on COVID-19. *Adv Mater Technol*. 2023;8(15):11.
18. Dai JY, Meng JP, Zhao XM, et al. A wearable self-powered multi-parameter respiration sensor. *Adv Mater Technol*. 2023;8(7):9.
19. Ning C, Cheng RW, Jiang Y, et al. Helical fiber strain sensors based on triboelectric nanogenerators for self-powered human respiratory monitoring. *ACS Nano*. 2022;16(2):2811-2821.
20. Zou Y, Gai Y, Tan P, et al. Stretchable graded multichannel self-powered respiratory sensor inspired by shark gill. *Fundam Res*. 2022;2(4):619-628.
21. Su YJ, Chen GR, Chen CX, et al. Self-powered respiration monitoring enabled by a triboelectric nanogenerator. *Adv Mater*. 2021;33(35):2101262.
22. Zhang BS, Tang YJ, Dai RR, et al. Breath-based human-machine interaction system using triboelectric nanogenerator. *Nano Energy*. 2019;64(7):103953.
23. Yeh MP, Adams TD, Gardner RM, Yanowitz FG. Turbine flowmeter vs. Fleisch pneumotachometer: a comparative study for exercise testing. *J Appl Physiol*. 1987;63(3):1289-1295.
24. von Kármán T, Rubach H. The mechanism of the fluid and air-resistense. *Phys Z*. 1912;13:49-59.
25. Fan FR, Tian ZQ, Wang ZL. Flexible triboelectric generator! *Nano Energy*. 2012;1(2):328-334.
26. Wang ZL. Triboelectric nanogenerators as new energy technology for self-powered systems and as active mechanical and chemical sensors. *ACS Nano*. 2013;7(11):9533-9557.
27. Wang XD, Song JH, Liu J, Wang ZL. Direct-current nanogenerator driven by ultrasonic waves. *Science*. 2007;316(5821):102-105.
28. Wu Y, Li Y, Zou Y, et al. A multi-mode triboelectric nanogenerator for energy harvesting and biomedical monitoring. *Nano Energy*. 2022;92:106715.

29. Gai YS, Wang EG, Liu MH, et al. A self-powered wearable sensor for continuous wireless sweat monitoring. *Small Methods*. 2022;6(10):2200653.
30. Dai JY, Li LL, Shi BJ, Li Z. Recent progress of self-powered respiration monitoring systems. *Biosens Bioelectron*. 2021;194:113609.
31. Tan PC, Han X, Zou Y, et al. Self-powered gesture recognition wristband enabled by machine learning for full keyboard and multicommand input. *Adv Mater*. 2022;34(21):2200793.
32. Xi Y, Cheng SJ, Chao SY, et al. Piezoelectric wearable atrial fibrillation prediction wristband enabled by machine learning and hydrogel affinity. *Nano Res*. 2023;16(9):11674-11681.
33. Von Karman T. Über den Mechanismus des Widerstandes, den ein bewegter Körper in einer Flüssigkeit erfährt. *Nachr Ges Wiss Goettingen Math Phys Kl*. 1911;1911:509-517.
34. Wang ZL. On Maxwell's displacement current for energy and sensors: the origin of nanogenerators. *Mater Today*. 2017;20(2):74-82.
35. Wu CS, Wang AC, Ding WB, Guo HY, Wang ZL. Triboelectric nanogenerator: a foundation of the energy for the new era. *Adv Energy Mater*. 2019;9(1):1802906.
36. Wang S, Fang YL, He H, Zhang L, Li CA, Ouyang JY. Wearable stretchable dry and self-adhesive strain sensors with conformal contact to skin for high-quality motion monitoring. *Adv Funct Mater*. 2021;31(5):2007495.
37. Lo LW, Zhao JY, Aono K, et al. Stretchable sponge electrodes for long-term and motion-artifact-tolerant recording of high-quality electrophysiologic signals. *ACS Nano*. 2022;16(8):11792-11801.
38. Halson SL. Monitoring training load to understand fatigue in athletes. *Sports Med*. 2014;44(S2):139-147.
39. Close RI. Dynamic properties of mammalian skeletal-muscles. *Physiol Rev*. 1972;52(1):129.
40. Zhang ZH, Lin SD, Luo W, et al. *Sox6* differentially regulates inherited myogenic abilities and muscle fiber types of satellite cells derived from fast- and slow-type muscles. *Int J Mol Sci*. 2022;23(19):11327.
41. Guyon I, Elisseeff A. An introduction to variable and feature selection. *J Mach Learn Res*. 2003;3(March):1157-1182.

SUPPORTING INFORMATION

Additional supporting information can be found online in the Supporting Information section at the end of this article.

How to cite this article: Xue Z, Tan P, Xue J, et al. Adaptive respiratory muscle trainer based on hybrid nanogenerator sensor and artificial intelligence. *InfoMat*. 2025;7(6):e70004. doi:10.1002/inf2.70004